OncoTargets and Therapy

Dovepress
open access to scientific and medical research

Open Access Full Text Article

ORIGINAL RESEARCH

RNA-Seq Profiling of Circular RNAs and the Oncogenic Role of circPVT1 in Cutaneous Squamous Cell Carcinoma

This article was published in the following Dove Press journal:
OncoTargets and Therapy

Shuang Chen
Junli Ding
Yunlin Wang
Tao Lu
Lili Wang
Xinghua Gao
Hongduo Chen
Le Qu
Chundi He

Department of Dermatology, No.1 Hospital of China Medical University, Hospital of China Medical University, Key Laboratory of Immunohematology, Shenyang, Liaoning, People's Republic of China

Background: Cutaneous squamous cell carcinoma (CSCC) is associated with a poor 5-year survival rate. circRNAs have an important role in a number of physiological and pathological processes. However, the relationship between circRNAs and cutaneous squamous cell carcinoma (CSCC) is unclear.

Purpose: The aim of the present study was to investigate the expression of circRNAs in cutaneous squamous cell carcinoma (CSCC) and its effect on CSCC proliferation and metastasis.

Methods: We used high-throughput sequencing (RNA-seq) to identify circRNAs that were differentially in CSCC tissue and their paracarcinoma tissue. Quantitative real-time PCR results confirm deep-sequencing findings in CSCC tissue and cell lines. CCK-8 assay and flow cytometry were used to detect the effect of circPVT1 on the proliferation and migration of CSCC cells.

Results: We identified 449 circRNAs that were differentially expressed between CSCC and normal adjacent tissue samples. circPVT1 (hsa_circ_0001821) was further researched to confirm its oncogene role in CSCC.

Conclusion: Differentially expressed circular RNA plays an important role in the development of CSCC, and circPVT1 may be an important target for the treatment of CSCC.

Keywords: circRNA, RNA-seq, CSCC, circPVT1

Introduction

Cutaneous squamous cell carcinoma (CSCC) accounts for up to 20% of all mortality linked to skin cancer, and is the 2nd leading form of malignant skin cancer.[1] There have been many advances in diagnosing and surgically treating CSCC, but once regional lymphatic metastasis or distant metastasis occurs, the 10-year survival rate of CSCC patients will drop below 20%.[2,3] As such, there is a clear need to more fully explore the molecular mechanisms governing the occurrence and development of this cancer, and to identify relevant therapeutic and/or diagnostic biomarkers of this disease.

Circular RNAs (circRNAs) were first identified based upon electron microscopic studies of virions.[4] However, more recent advances in high-throughput sequencing have revealed these circRNAs to be present at very high levels, evolutionarily conserved, and to be expressed stably in tissues in a manner specifically associated with developmental stage.[5,6] These circRNAs exhibit distinct roles in many different types of human disease, including neurological disorders,[7]

Correspondence: Chundi He; Le Qu
Department of Dermatology, No.1 Hospital of China Medical University, Key Laboratory of Immunodermatology, 155 North Nanjing Street, Shenyang, Liaoning 110001, People's Republic of China
Tel/Fax +86-24-83282999
Email cdhe@cmu.edu.cn; 317224999@qq.com

submit your manuscript | www.dovepress.com
DovePress
http://doi.org/10.2147/OTT.S252233

heart disease[8] and cancer.[9–11] These circRNAs can execute a number of biological functions, including serving as molecular sponges that sequester microRNAs (miRNAs).[12,13] Other circRNAs can also function by directly binding specific RNA-binding proteins, thereby controlling their activity[14,15] and altering their biological functionality.[16–18] Despite these findings, our understanding of how circRNAs function in CSCC is limited.

In the present study, we conducted circRNAs sequencing in 3 pairs of CSCC and matched control tissues with the goal of identifying CSCC-specific circRNAs profiles. Of those identified differentially expressed circRNAs, circPVT1 (termed hsa_circ_0001821 in circbase[19]), originating from Exon 2 of the PVT1 gene (chr8: 128,902,834 −128,903,244 strand: +) which was 410 nucleotides long following splicing, was of particular interest. Previous reports have shown circPVT1 to play an oncogenic role in gastric cancer, head and neck tumors, and non-small cell lung cancer via serving as a miRNA sponge.[20–22] The role of this circRNAs in CSCC, however, was not previously examined. We, therefore, conducted loss-of-function experiments assessing the oncogenic role of cirPVT1 in CSCC. In summary, our results suggest that targeting circPVT1 may be a viable therapeutic strategy worthy of future examination.

Materials and Methods

Clinical Specimens

A total of 30 pairs of CSCC tumor tissues and adjacent healthy tissue were collected from patients undergoing surgery, and samples were stored at-80 °C. This study received the approval of the ethics committee of the first affiliated Hospital of China Medical University, and all patients provided informed consent. CSCC had been pathologically diagnosed in all patients, and no patients had undergone radio- or chemotherapy at time of sample collection.

RNA Preparation

TRIzol (Thermo Fisher Scientific, MA, USA) was used to isolate total RNA, and then a Qubit 3.0 Fluorometer (Invitrogen, CA, USA) was used to gauge RNA concentrations, and an Agilent 2100 Bioanalyzer (Applied Biosystems, CA, USA) was used to approximate RNA integrity. Only samples that had a minimum RIN value of 7.0 underwent additional processing.

Library Construction and High-Throughput Sequencing

We prepared a library for RNA sequencing using 2μg of total RNA and a KAPA RNA HyperPrep Kit with RiboErase (HMR) for Illumina® (Kapa Biosystems, Inc., MA, USA). Initially, DNA probe hybridization was conducted in order to remove rRNA from samples, after which remaining RNA was combined with 10 U of RNase R (Epicentre Technologies, WI, USA) for 30 min at 37°C, followed by purification using VAHTS RNA Clean Beads. The remaining RNA samples then underwent fragmentation followed by first strand and directional second strand synthesis reactions. Next, A tailing and adapter ligation were conducted using the purified cDNA, and the adapter-ligated DNA then underwent amplification. A DNA 1000 chip was next used to gauge the concentration and quality of the resultant library using an Agilent 2100 Bioanalyzer. Prior to sequencing, additional library quantification was conducted with the qPCR-based KAPA Biosystems Library Quantification kit (Kapa Biosystems). Finally, libraries were diluted to 10 nM and pooled in equimolar amounts before clustering. Paired-End 150 (PE150) sequencing was conducted using an Illumina Hiseq Xten platform.

Bioinformatics Analysis

RNA-seq data were first mapped to the latest UCSC transcript set with Bowtie2 v 2.1.0,[23] and RSEM v1.2.15[24] was used to estimate levels of gene expression. TMM (trimmed mean of M-values) was employed for normalizing gene expression, after which edgeR[25] was used to identify differentially expressed genes, which included those with a $p < 0.05$ and a >2-fold change. When assessing the expression of circRNAs, STAR[26] was used to map reads to the genome, while DCC[27] was used for circRNA identification and estimation of expression. Gene ontology (GO) and KEGG pathway analyses were conducted using ClusterProfiler R. circRNAs miRNA targets were predicted using MiRanda (V3.3). Cytoscape (V3.7.1) was for mapping a potential circRNA-miRNA-mRNA interaction network.

Cell Culture

Human HaCat, A431, SCL-1, and SCL-12 were from the Cell Bank of Chinese Academy of Sciences (Shanghai, China). Cells were grown in DMEM with 10% FBS and penicillin/streptomycin at 37 C with 5% CO_2.

qRT-PCR

TRIzol (Thermo Fisher Scientific) was used for extraction of CSCC tissue and cell total RNA, after which 1 ug or RNA was reverse transcribed using the Geneseed First Strand cDNA Synthesis Kit (Geneseed, Guangzhou, China). For qRT-PCR reactions, SYBR Green Master Mix (Geneseed) was utilized on an ABI 7500 system. GAPDH was used for normalizing gene expression, with relative circRNA expression determined via the $2^{-\Delta\Delta CT}$ method. Primers were generated by Sangon (Shanghai, China), and were as follows: circPVT1-F: 5′-ttgggtctccctatggaatg-3′, circPVT1-R:5′-gccaaaagatcaggcct-caa-3′;linear-PVT1-F: 5′-TCTGGGGAATAACGCTGGT G-3′, linear-PVT1-R: 5′-CAGCCACAGCCTCCCTTAA A-3′; GAPDH-F:5′-GCCGTCTAGAAAAACCTGCC-3′, GAPDH-R: 5′-CCACCTGGTGCTCAGTGTAG-3′.

siRNA Transfection

The following siRNA was used to knock down circPVT1 expression: 5′-GCUUGAGGCCUGAUCUUU UTT-3′ (GenePharma, Shanghai, China). Lipofectamine 2000 (Thermo Fisher Scientific) was used for transfection based on provided directions.

CCK-8 Assay

A total of 3×10 3 cells were added to each well of 96-well played following transfection. Cells were allowed to incubate for 24, 48, or 72 h, after which 10 ul WST-8 was added per well, and a CCK-8 kit (Dojindo, Kumamoto, Japan) was used to assess viability.

Flow Cytometry

An Annexin V-FITC Apoptosis Detection Kit (KeyGen Biotech, Nanjing, China) was used based on provided instructions. Briefly, at 48 h post-transfection cells were collected and stained using Annexin V-FITC/PI, after which they were analyzed flow cytometrically on a FACS Canto II machine (BD Biosciences). BD FACSDiva and FCS Express 5 (De Novo Software, CA, USA) were used for data analyses.

Migration and Invasion Assays

A transwell chamber was used for migration assays, while this same chamber was pre-coated with matrigel in order to conduct invasion assays, consistent with manufacturer directions (BD Science, Bedford, MA, USA).

Cells (5×10 4 cells/100mL serum-free medium) were added to the upper portion of the well for 48 h, after which three random fields were imaged in order to quantify rates of cell migration and invasion based on counts of the total number of cells observed exhibiting these behaviors.

Statistical Analyses

GraphPad Prism 7.0 was used for all analyses. Data are means ± SD. Significance between groups was compared via paired and two-tailed Student's t-tests, while two-way ANOVAs were used when more than two groups of data were being compared. $P<0.05$ was the significance threshold.

Results

Patterns of Differential circRNA Expression in CSCC

We began by conducting high-throughput sequencing in order to identify circRNAs that were differentially expressed in 3 pairs of CSCC and adjacent normal tissues. This analysis identified 10,669 distinct circRNA molecules, with the distribution of this circRNAs across chromosomes generated presented in a Circos plot (Figure 1A). Following conditional filtering ($p<0.05$ and Fold change>2.0), we identified 449 circRNAs that were differentially expressed between CSCC and normal adjacent tissue samples, with 393 and 55 being up- and downregulated in CSCC samples, respectively. We then generated a hierarchically clustered heatmap of these circRNA expression profiles (Figure 1B). A volcano plot highlighting the significance of differentially expressed circRNAs was also generated (Figure 1C).

GO and Pathway Enrichment Analyses

We next conducted a GO analysis in order to annotate the functions of host genes for identified differentially expressed circRNAs, with the top 30 enriched GO terms shown in Figure 2A. The top GO terms relating to biological processes included DNA replication, endosomal transport, and nucleic acid transport, while the top cellular component terms were focal adhesion, cell−substrate adherens junction, and lamellipodium, and the top molecular function GO terms were guanylnucleotide exchange factor activity, magnesium ion binding, and Ras guanyl-nucleotide exchange factor activity.

We additionally conducted KEGG pathway analyses to further explore the functionality of the host genes for

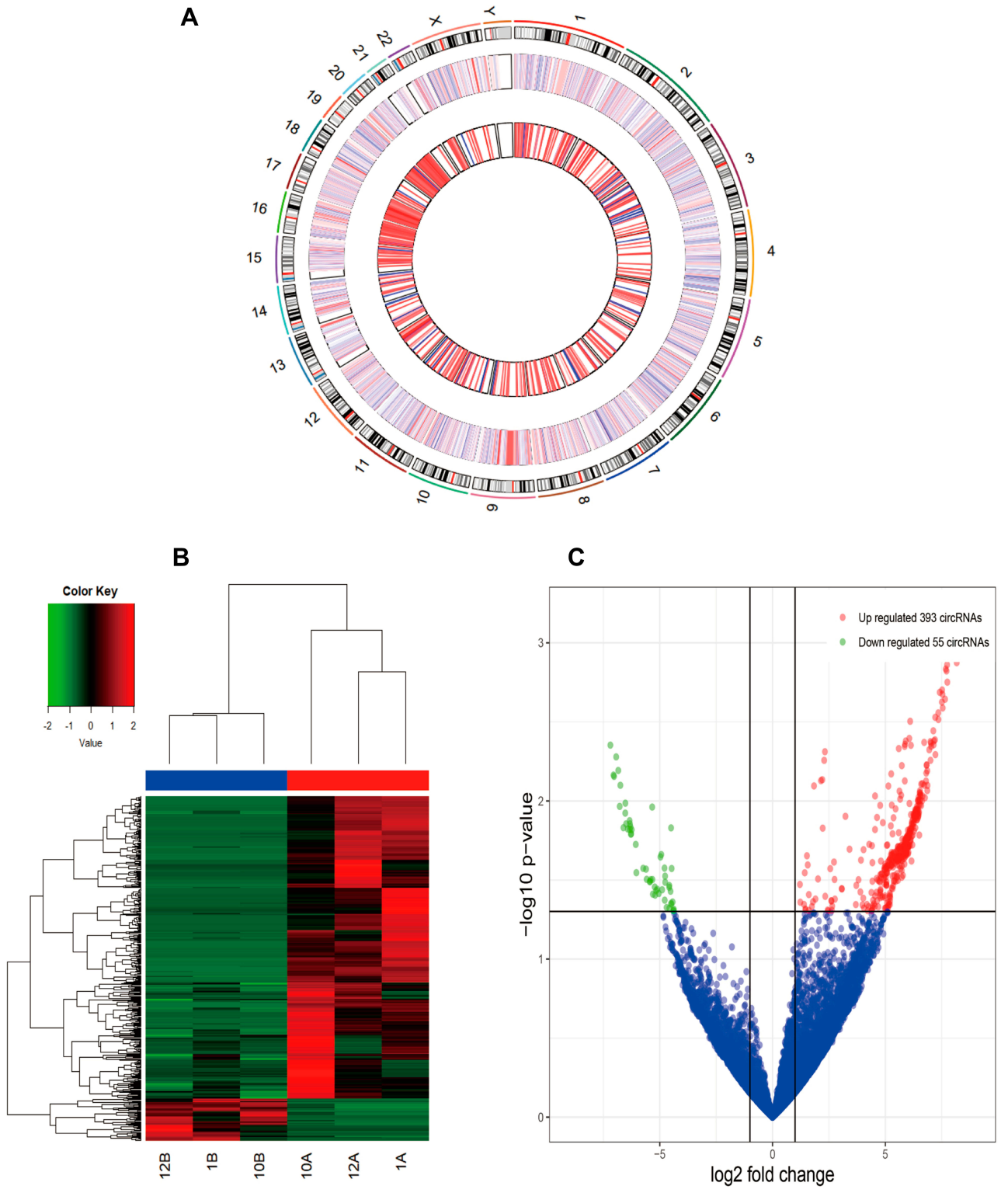

Figure 1 Global differentially expressed circRNAs characteristics in human CSCC. (**A**) Circos plot highlighting differentially expressed circRNAs in human chromosomes. (**B**) Hierarchical clustering analysis of differentially expressed circRNAs in CSCC, with rows corresponding to tissue samples and columns corresponding to particular circRNAs. (**C**) A volcano plot comparing the significance of differentially expressed circRNAs between groups, with the horizontal and vertical axes corresponding to FC values and p-values for the identified circRNAs, respectively. Red and green dots correspond to circRNAs that were significantly up- or down-regulated, respectively (FC > 2.0 and p < 0.05).

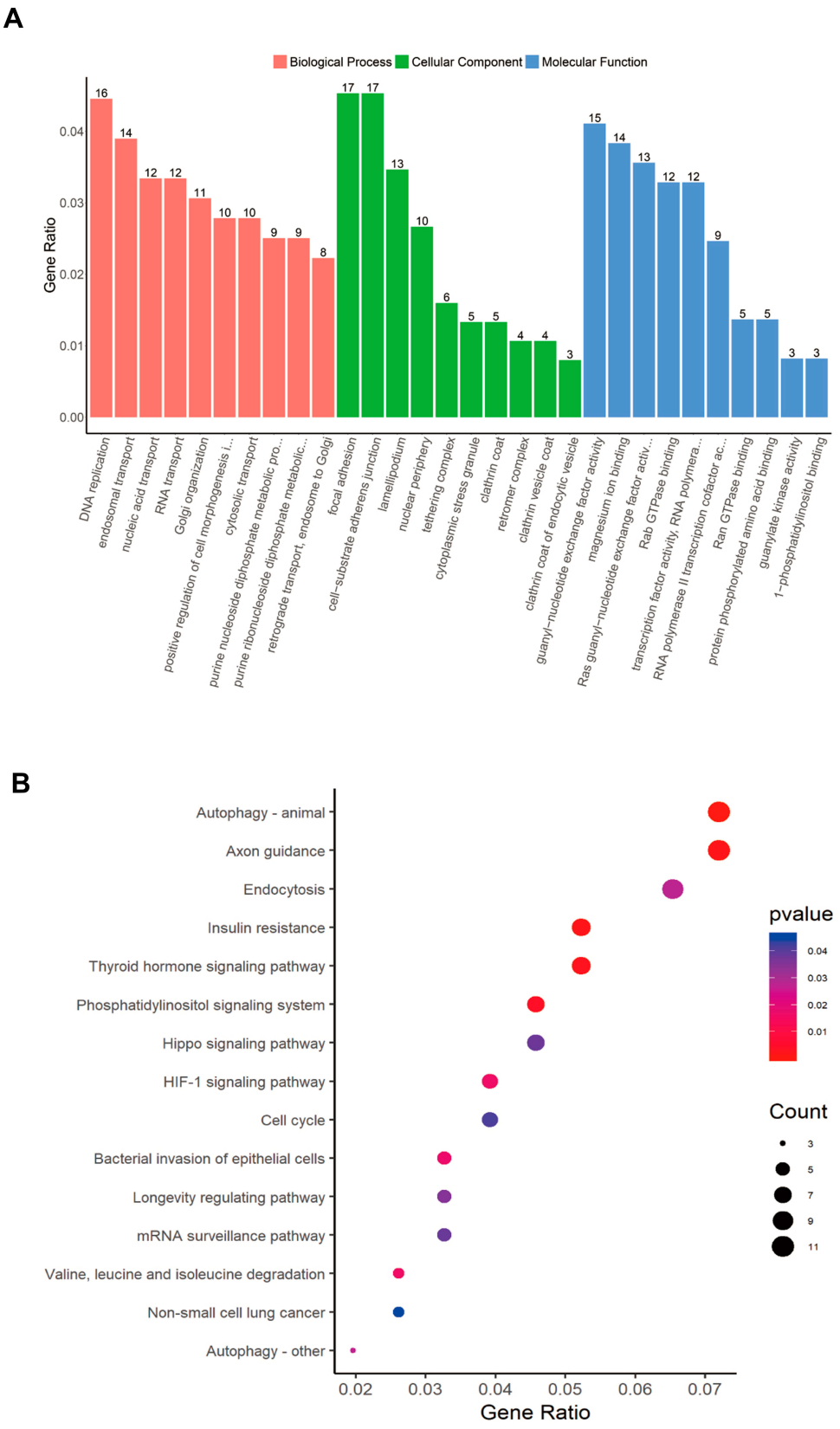

Figure 2 GO and pathway enrichment analyses for differentially expressed circRNA host genes in CSCC. (**A**) Top 30 enriched GO terms for differentially expressed circRNA host genes. (**B**) Top 15 enriched KEGG terms for differentially expressed circRNA host genes.

differentially expressed circRNAs, with the top 15 enriched pathways shown in Figure 2B. The most enriched pathway identified was autophagy – animal.

Construction of a circRNA-miRNA-mRNA Network

Previous studies have shown that circRNAs can serve as effective miRNA sponges, sequestering these molecules to inhibit their ability to control downstream target gene expression. As such, we next constructed a circRNA-miRNA-mRNA interaction network based on our sequencing results. For this network, we chose the top 10 differentially expressed circRNAs, and we then predicted the associated target miRNAs and mRNAs using Miranda 3.3 (Figure 3A). The specific regulatory network for hsa_circ_0001821 is shown in Figure 3B. Overall, these networks offered insights into the regulatory mechanisms whereby dysregulated circRNAs may influence CSCC.

Elevated circPVT1 Expression in CSCC Tissues and Cells

Our sequencing data suggested that circPVT1 exhibited a 5-fold increase in expression in CSCC tissues relative to adjacent normal tissues. We then further confirmed this finding via qRT-PCR in 30 pairs of CSCC and normal paracancerous tissue (Figure 4A), and we further observed elevated circPVT1 expression in the A431, SCL1, and SCL12 cell lines relative to normal control cells (Figure 4B). We next confirmed the backspliced site sequences of RT-PCR products via Sanger Sequencing (Figure 4C), with the results proving to be consistent with cyclization sites included in circbase database (http://www.circbase.org/). Convergent and divergent primers were then designed so as to amplify linear PVT1 and circPVT1, respectively. These pairs of primers were used individually to amplify A431 and SCL-1 cell line cDNA and gDNA, with circPVT1 only being amplified in cDNA samples using divergent primers. Divergent primers failed to amplify any gDNA products (Figure 4D). We further confirmed via qRT-PCR that circPVT1 was RNase R resistant, whereas linear PVT1 was rapidly degraded upon RNase R treatment (Figure 4E)

circPVT1 Knockdown Inhibits CSCC Cell Migration and Invasion

To explore the functional role of circPVT1 in CSCC, we next knocked down this circRNA via transducing A431 and SCL-1 cells with circPVT1-specific siRNA constructs. We then confirmed that these siRNA constructs, which targeted the circPVT1 junction site, significantly decreased endogenous circPVT1 levels in SCL-1 cells (Figure 5A). A CCK-8 assay demonstrated that knocking down circPVT1 markedly impaired the proliferation of CSCC cells relative to control cells (Figure 5B). We next explored how circPVT1 influenced SCL-1 cell apoptosis via flow cytometry, revealing a significant increase in the apoptotic death of these cells upon circPVT1 knockdown (Figure 5C). In addition, circPVT1 knockdown suppressed SCL-1 cell migration and invasion in vitro in a series of Transwell assays (Figure 5D).

Discussion

circRNAs contain a covalent closed loop structure, lacking both terminal poly-A tails and caps on the 3′ and 5′ ends, respectively.[28,29] These non-coding RNAs have been a topic of increasing research interest in recent years,[30] and advances in sequencing technologies have led to the discovery of increasing numbers of circRNAs that are dysregulated in a wide range of cancer subtypes,[31–34] These circRNAs have been found to play central roles in regulating the expression of specific target genes. However, the specific role of circRNAs in CSCC has only been examined in a limited number of studies to date.[8,35] In this report, we screened for circRNAs that were differentially regulated between CSCC tumor and adjacent normal control tissues using RNA-seq datasets, leading us to identify thousands of circRNAs expressed in these tissues. Of the detected circRNAs, we specifically focused on circPVT1, which was elevated in CSCC tissues and cells. When we knocked down circPVT1, we found that this resulted in the apoptotic death of CSCC cells and impaired their ability to proliferate, migrate, and invade. While these results highlight the potential relevance of circPVT1 in CSCC, further research will be needed to fully clarify the associated molecular mechanisms governing the observed phenotypes.

To begin to explore such mechanisms, we utilized the miRanda tool to predict miRNAs that may bind to circPVT1, highlighting a number of distinct miRNAs with which circPVT1 may be able to bind, serving as a sponge that competes for these miRNAs and reduces their ability to interact with lncRNAs and mRNA targets. It is worth noting that Verduci et al and Qin et al, respectively, found that circPVT1 can serve as a sponge for miR-497 in head and neck squamous cell carcinoma (HNSCC) and non-small cell lung cancer (NSCLC).[20,21] Moreover, in a

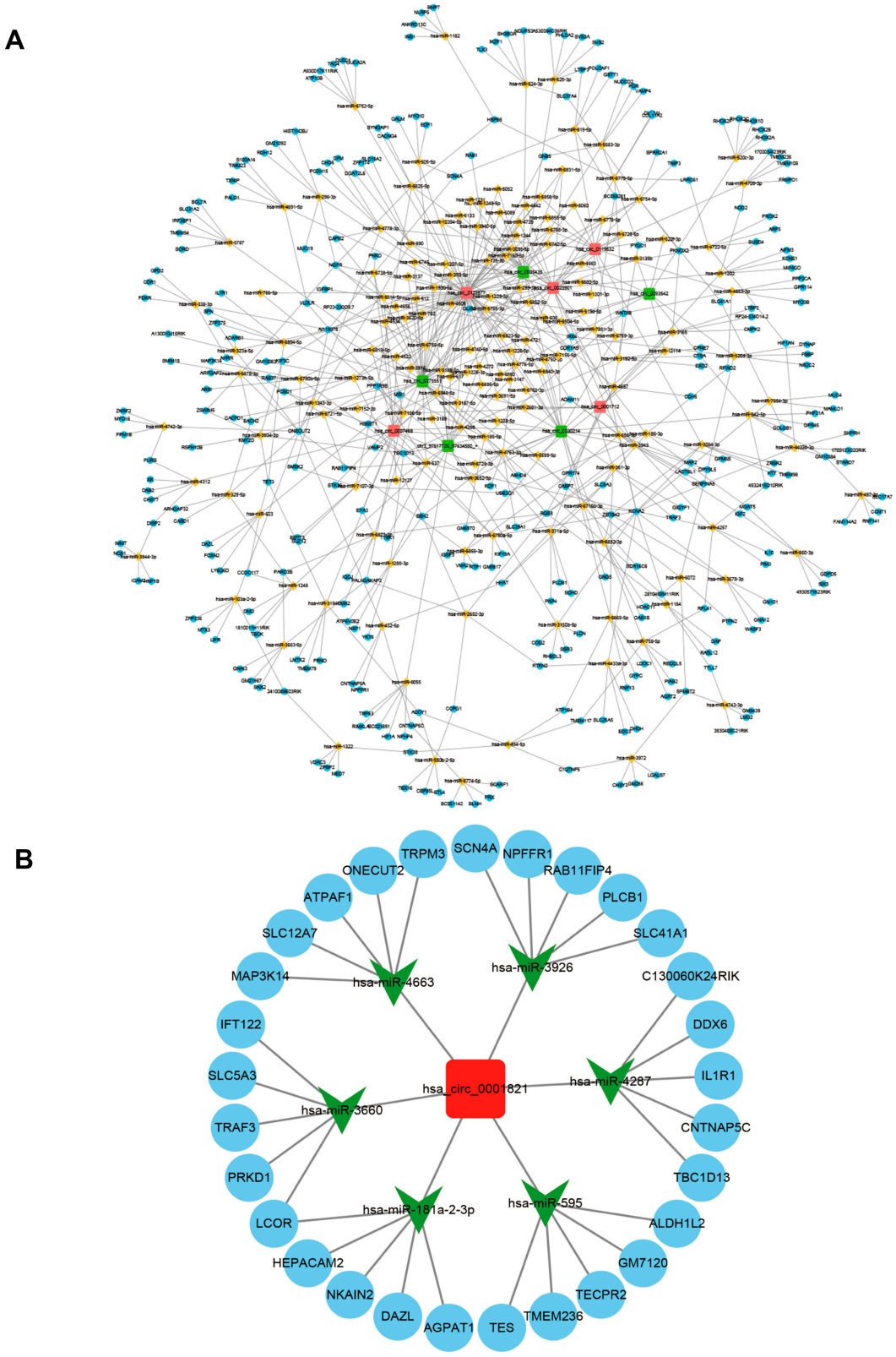

Figure 3 circRNA–miRNA-mRNA interaction network. (**A**) A regulatory network for the top 10 most significantly differentially expressed circRNAs. (**B**) The hsa_circ_0001821 (circPVT1) regulatory network, with a red square marking hsa_circ_0001821, a green triangle marking the miRNAs interacting with hsa_circ_0001821, and a blue circle marking miRNA target genes.

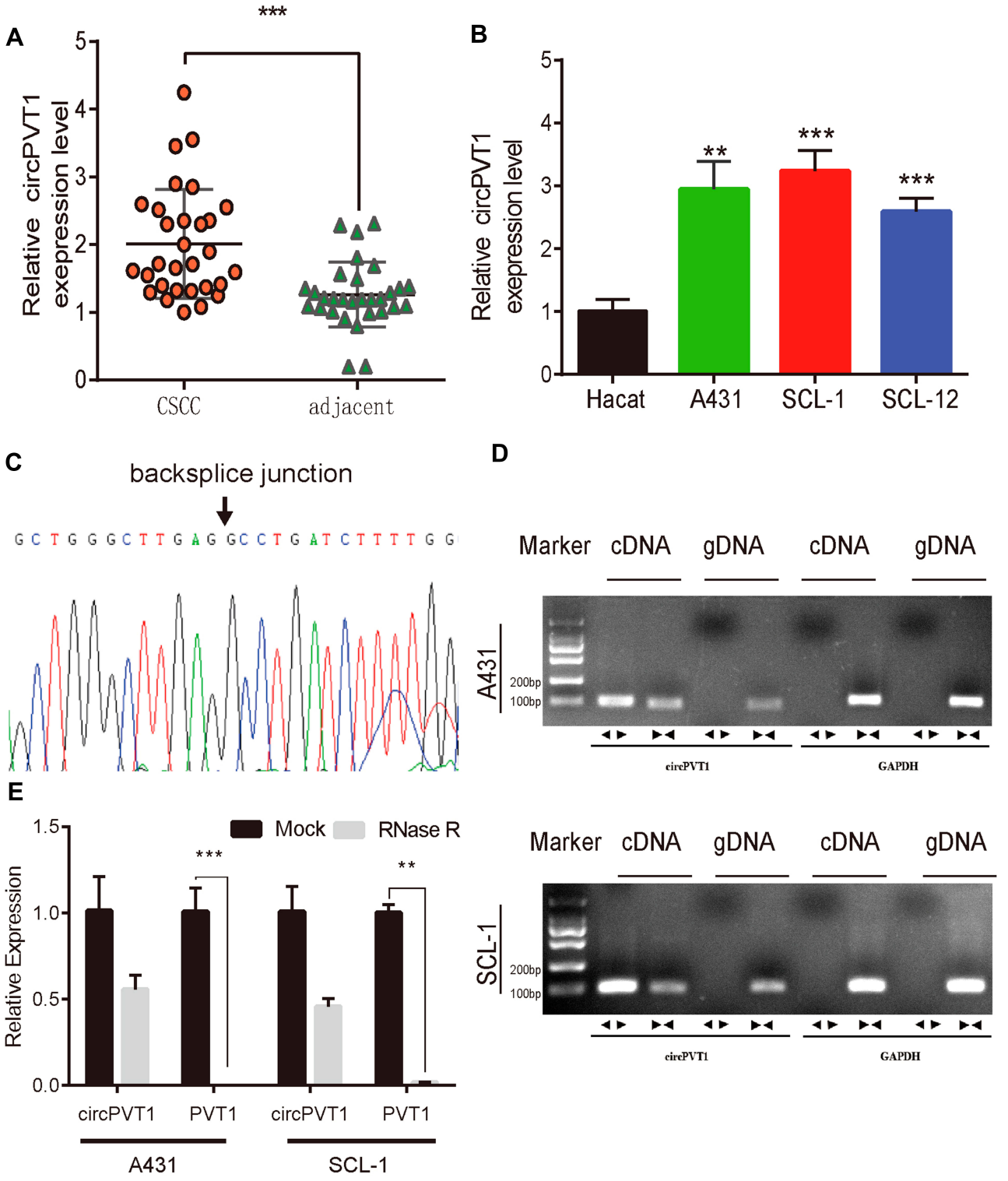

Figure 4 Validation and assessment of circPVT1 expression in. (**A**) qRT-PCR was used to confirm that there was elevated circPVT1 expression in CSCC tissues relative to adjacent normal tissue. Data are means ± SD (n=30). (**B**) Relative circPVT1 expression in HaCAT cells and CSCC cell lines (A431, SCL-1, SCL-12) as measured via qRT-PCR. **P<0.01, ***P<0.001. (**C**) The circPVT1 junction site was confirmed via RT-PCR and Sanger sequencing. (**D**) circPVT1 expression in A431 and SCL-1 cells was confirmed via RT–PCR. Levels of circPVT1 specifically in cDNA were amplified using divergent primers, leaving gDNA levels unamplified. GAPDH was a negative control. (**E**) circPVT1 was more tolerant of RnaseR degradation than was PVT1 mRNA in A431 and SCL-1 cells.

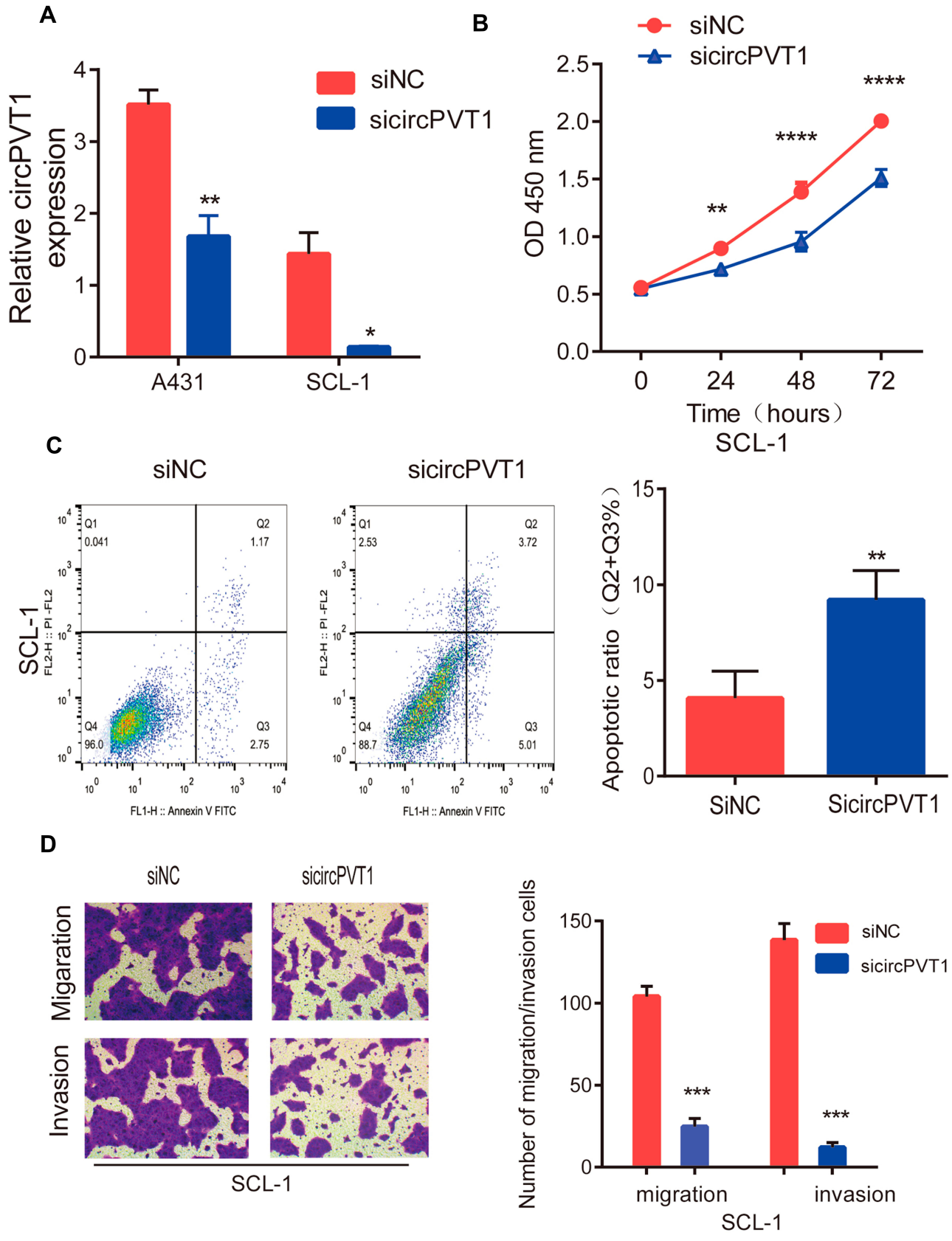

Figure 5 Knocking down circPVT1 inhibits CSCC cell proliferation, migration, and invasion. (**A**) A431 and SCL-1 cells were transfected with a circPVT1-specific siRNA, with qRT-PCR used to confirm knockdown. Data are mean ± SD, *P<0.05, **P<0.01. (**B**) A CCK-8 assay was conducted in SCL-1 cells. **P<0.01, ****P<0.0001. (**C**) Apoptosis analysis in SCL-1 cells. **P<0.01. (**D**) The migration and invasion of A431 and SCL-1 cells was assessed following sicircPVT1 or siNC transfection. Cells that had migrated or invaded successfully were imaged and quantified. Data are means ± SD (n=3). ×200 magnification. ***P<0.001.

study of CSCC by Wei et al, researchers found that the expression of miR-497 in CSCC tissue samples was lower than that in normal tissues, and that it was able to promote the progression of CSCC by targeting FAM114A2.[36] In another study of CSCC, Mizrahi et al found that miR-497 was underexpressed in CSCC tissues and that it induces reversion of the epithelial to mesenchymal transition (EMT).[37] These previous studies have shown that the interaction between circPVT1 and miR-497 may play an important role in the progression of CSCC. In addition, we searched the miRNA combined hsa_circ_0001821 in the CircInteractome database,[38] revealing intersections with miRanda prediction results (Figure 6A). Through this approach, we found that only hsa-miR-587 was identified by these two algorithms. However, we found no evidence of the combination of hsa _ circ _ 0001821 and hsa-miR-497 in CircInteractome and miRanda prediction results. This may be due to the different prediction approaches employed by our team and past research teams.

Our current research is limited by its lack of mechanistic studies and due to limitations of experimental facilities, our current research lacks in vivo experimental evidence, which may let us better understand the oncogene role of circPVT1 in CSCC. Further studies of the interaction between miR-497/miR-587 and circPVT1 will be a focus of our future research. Moreover, as several circular RNAs have been reported to be translatable,[16,18,39–41] we evaluated the translational potential of has_circ_0001821. In the Circbank database,[42] we found that hsa_circ_0001821 had an

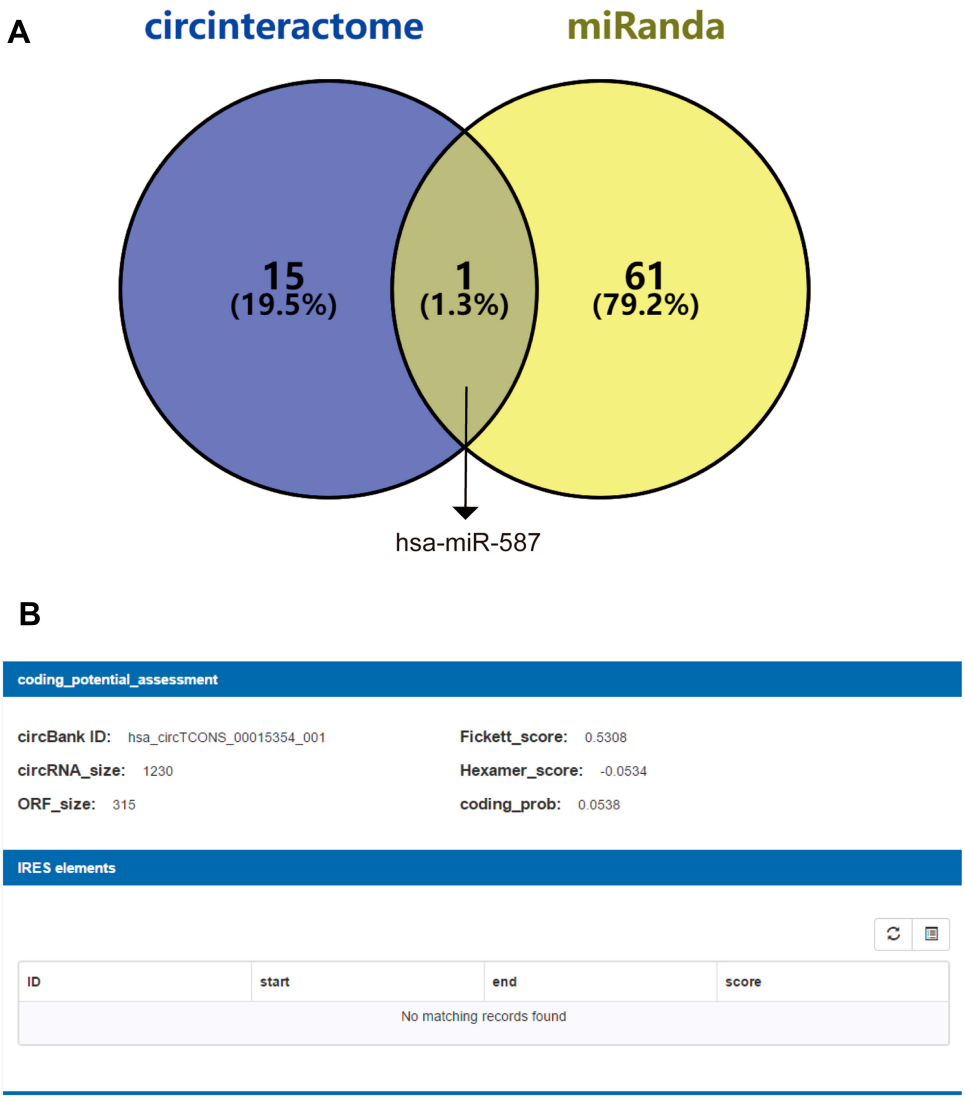

Figure 6 Prediction of the miRNAs interacting with circPVT1and its translation potential. (**A**) Intersection of CircInteractome database and miRanda software prediction results. (**B**) Prediction of circPVT1 (hsa_circ_0001821) ORF and IRES sequences.

open reading frame of 315bp in size, but there was no internal ribosome entry site (IRES), suggesting that hsa_circ_0001821 could not be translated (Figure 6B). As such, future experiments should focus on following up on these predictive results in order to identify the specific target miRNAs through which circPVT1 exerts its effects in CSCC.

Conclusion

In summary, we were able to identify patterns of differential circRNA expression profiles between CSCC and adjacent control tissues. We found that several circRNAs were aberrantly expression in CSCC, and that circPVT1 functioned in an oncogenic manner in CSCC. While we have not yet fully clarified the molecular mechanisms underlying the role of circPVT1 in CSCC, our results highlight its potential as a therapeutic target in this disease.

Data Sharing Statement

The data used and analyzed during the current study are available from the corresponding author on reasonable request.

Ethics Approval and Consent to Participate

Informed consent was obtained from all individual participants included in the present study. The present study was approved by the Ethics Committee of the NO.1 Hospital of China Medical University.

Acknowledgments

The authors would like to acknowledge the Key Laboratory of Immunodermatology, Ministry of Health (China Medical University. Shenyang, China) for providing the space and equipment for conducting the experiments.

Funding

This work was supported by grants from the Science & Technology Fund of Liaoning Province (grant no. 201501013) and the Distinguished Professor Foundation of Liaoning Province (grant no. Liao [2012] 145).

Disclosure

The authors report no conflicts of interest in this work.

References

1. Wang A, Landén NX, Meisgen F, et al. MicroRNA-31 is overexpressed in cutaneous squamous cell carcinoma and regulates cell motility and colony formation ability of tumor cells. *PloS One*. 2014;9(7):e103206.
2. Ogata D, Tsuchida T. Systemic immunotherapy for advanced cutaneous squamous cell carcinoma. *Curr Treat Options Oncol*. 2019;20(4):30.
3. Wang Y, Bensen S, Wen X, et al. The roles of lncRNA in cutaneous squamous cell carcinoma. *Front Oncol*. 2020;10:158.
4. Sanger HL, Klotz G, Riesner D, Gross HJ, Kleinschmidt AK. Viroids are single-stranded covalently closed circular RNA molecules existing as highly base-paired rod-like structures. *Proc Natl Acad Sci U S A*. 1976;73(11):3852–3856.
5. Jeck WR, Sorrentino JA, Wang K, et al. Circular RNAs are abundant, conserved, and associated with ALU repeats. *RNA*. 2013;19(2):141–157.
6. Rybak-Wolf A, Stottmeister C, Glažar P, et al. Circular RNAs in the mammalian brain are highly abundant, conserved, and dynamically expressed. *Mol Cell*. 2015;58(5):870–885.
7. Sang Q, Liu X, Wang L, et al. CircSNCA downregulation by pramipexole treatment mediates cell apoptosis and autophagy in parkinson's disease by targeting miR-7. *Aging*. 2018;10(6):1281–1293.
8. Sand M, Bechara FG, Gambichler T, et al. Circular RNA expression in cutaneous squamous cell carcinoma. *J Dermatol Sci*. 2016;83(3):210–218.
9. Yang Z, Qu CB, Zhang Y, et al. Dysregulation of p53-RBM25-mediated circAMOTL1L biogenesis contributes to prostate cancer progression through the circAMOTL1L-miR-193a-5p-Pcdha pathway. *Oncogene*. 2019;38(14):2516–2532.
10. Cheng Z, Yu C, Cui S, et al. circTP63 functions as a ceRNA to promote lung squamous cell carcinoma progression by upregulating FOXM1. *Nat Commun*. 2019;10(1):3200.
11. Li B, Wang F, Li X, Sun S, Shen Y, Yang H. Hsa_circ_0008309 may be a potential biomarker for oral squamous cell carcinoma. *Dis Markers*. 2018;2018(undefined):7496890.
12. Hansen TB, Jensen TI, Clausen BH, et al. Natural RNA circles function as efficient microRNA sponges. *Nature*. 2013;495(7441):384–388.
13. Kristensen LS, Hansen TB, Venø MT, Kjems J. Circular RNAs in cancer: opportunities and challenges in the field. *Oncogene*. 2018;37(5):555–565.
14. Huang JZ, Chen M, Chen D, et al. A peptide encoded by a putative lncRNA HOXB-AS3 suppresses colon cancer growth. *Mol Cell*. 2017;68(1):171–184.e176.
15. Du WW, Yang W, Li X, et al. A circular RNA circ-DNMT1 enhances breast cancer progression by activating autophagy. *Oncogene*. 2018;37(44):5829–5842.
16. Zhang M, Zhao K, Xu X, et al. A peptide encoded by circular form of LINC-PINT suppresses oncogenic transcriptional elongation in glioblastoma. *Nature Commun*. 2018;9(1):4475.
17. Wang Y, Wang Z. Efficient backsplicing produces translatable circular mRNAs. *RNA*. 2015;21(2):172–179.
18. Zhang M, Huang N, Yang X, et al. A novel protein encoded by the circular form of the SHPRH gene suppresses glioma tumorigenesis. *Oncogene*. 2018;37(13):1805–1814.
19. Glažar P, Papavasileiou P, Rajewsky N. circBase: a database for circular RNAs. *RNA*. 2014;20(11):1666–1670.
20. Verduci L, Ferraiuolo M, Sacconi A, et al. The oncogenic role of circPVT1 in head and neck squamous cell carcinoma is mediated through the mutant p53/YAP/TEAD transcription-competent complex. *Genome Biol*. 2017;18(1):237. doi:10.1186/s13059-017-1368-y

21. Qin S, Zhao Y, Lim G, Lin H, Zhang X, Zhang X. Circular RNA PVT1 acts as a competing endogenous RNA for miR-497 in promoting non-small cell lung cancer progression. *Biomed Pharmacother*. 2019;111:244–250. doi:10.1016/j.biopha.2018.12.007
22. Chen J, Li Y, Zheng Q, et al. Circular RNA profile identifies circPVT1 as a proliferative factor and prognostic marker in gastric cancer. *Cancer Lett*. 2017;388(undefined):208–219.
23. Langmead B, Salzberg SL. Fast gapped-read alignment with bowtie 2. *Nat Methods*. 2012;9(4):357–359.
24. Li B, Dewey CN. RSEM: accurate transcript quantification from RNA-Seq data with or without a reference genome. *BMC Bioinf*. 2011;12(1):323.
25. Robinson MD, McCarthy DJ, Smyth GK. edgeR: a bioconductor package for differential expression analysis of digital gene expression data. *Bioinformatics*. 2010;26(1):139–140.
26. Lefort K, Brooks Y, Ostano P, et al. A miR-34a-SIRT6 axis in the squamous cell differentiation network. *EMBO J*. 2013;32(16):2248–2263.
27. Cheng J, Metge F, Dieterich C. Specific identification and quantification of circular RNAs from sequencing data. *Bioinformatics*. 2016;32(7):1094–1096.
28. Chen LL, Yang L. Regulation of circRNA biogenesis. *RNA Biol*. 2015;12(4):381–388.
29. Jeck WR, Sharpless NE. Detecting and characterizing circular RNAs. *Nature Biotechnol*. 2014;32(5):453–461.
30. Zheng LL, Li JH, Wu J, et al. deepBase v2.0: identification, expression, evolution and function of small RNAs, LncRNAs and circular RNAs from deep-sequencing data. *Nucleic Acids Res*. 2016;44(null):D196–D202.
31. Zhong Z, Lv M, Chen J. Screening differential circular RNA expression profiles reveals the regulatory role of circTCF25-miR-103a-3p/miR-107-CDK6 pathway in bladder carcinoma. *Sci Rep*. 2016;6:30919.
32. Yang Y, Gao X, Zhang M, et al. Novel role of FBXW7 circular RNA in repressing glioma tumorigenesis. *J Natl Cancer Inst*. 2018;110(3):undefined.
33. Xuan L, Qu L, Zhou H, et al. Circular RNA: a novel biomarker for progressive laryngeal cancer. *Am J Transl Res*. 2016;8(2):932–939.
34. Li F, Zhang L, Li W, et al. Circular RNA ITCH has inhibitory effect on ESCC by suppressing the Wnt/β-catenin pathway. *Oncotarget*. 2015;6(8):6001–6013.
35. An X, Liu X, Ma G, Li C. Upregulated circular RNA circ_0070934 facilitates cutaneous squamous cell carcinoma cell growth and invasion by sponging miR-1238 and miR-1247-5p. *Biochem Biophys Res Commun*. 2019;513(2):380–385. doi:10.1016/j.bbrc.2019.04.017
36. Wei XH, Gu XL, Zhou XT, Ma M, Lou CX. miR-497 promotes the progression of cutaneous squamous cell carcinoma through FAM114A2. *Eur Rev Med Pharmacol Sci*. 2018;22(21):7348–7355.
37. Mizrahi A, Barzilai A, Gur-Wahnon D, et al. Alterations of microRNAs throughout the malignant evolution of cutaneous squamous cell carcinoma: the role of miR-497 in epithelial to mesenchymal transition of keratinocytes. *Oncogene*. 2018;37(2):218–230.
38. Dudekula DB, Panda AC, Grammatikakis I, De S, Abdelmohsen K, Gorospe M. CircInteractome: a web tool for exploring circular RNAs and their interacting proteins and microRNAs. *RNA Biol*. 2016;13(1):34–42.
39. Pamudurti NR, Bartok O, Jens M, et al. Translation of CircRNAs. *Mol Cell*. 2017;66(1):9–21 e27. doi:10.1016/j.molcel.2017.02.021
40. Marín-Béjar O, Mas AM, González J, et al. The human lncRNA LINC-PINT inhibits tumor cell invasion through a highly conserved sequence element. *Genome Biol*. 2017;18(1):202.
41. Legnini I, Di Timoteo G, Rossi F, et al. Circ-ZNF609 is a circular RNA that can be translated and functions in myogenesis. *Mol Cell*. 2017;66(1):22–37 e29. doi:10.1016/j.molcel.2017.02.017
42. Liu M, Wang Q, Shen J, Yang BB, Ding X. Circbank: a comprehensive database for circRNA with standard nomenclature. *RNA Biol*. 2019;16(7):899–905.